Journal of Engineering Physics and Thermophysics, Vol. 81, No. 1, 2008

INFLUENCE OF THE PLASMA OF A HIGH-FREQUENCY BARRIER DISCHARGE ON THE STRUCTURE OF THE DYNAMIC BOUNDARY LAYER ON A FLAT SURFACE

O. G. Penyaz'kov, P. P. Khramtsov, M. Yu. Chernik, I. N. Shatan, and I. A. Shikh

UDC 533.9.082.5;537.523.2

Methods of obtaining a surface high-frequency barrier discharge have been analyzed. The results of investigation of the influence of this discharge on the characteristics of the dynamic boundary layer on a flat surface have been given.

Introduction. Active investigations on creation of a plasma flow ahead of a bluff body with the aim of reducing aerodynamic drag have been carried out in recent years. A detailed analysis of these experiments was made in [1, 2]. The results obtained found use in today's aircraft industry and triggered new developments in the field of application of a surface plasma toward increasing the economy and improving the controllability of aircraft in atmospheric flight by changing their aerodynamic characteristics [1].

The influence of spark discharges on the aerodynamic drag for supersonic speeds has been investigated in [3, 4]. Flow past a conic cylinder with an angle of opening of 30^{o} for Mach number M = 2 was observed. Models with diameters of 40 to 80 mm had a pointed electrode at the top for concentration of the electric field. A power supply with an output voltage of 5 kV, a carrier frequency of 13–16 MHz, and an amplitude modulation of 100 Hz was used. The results showed a reduction of up to 6% in the aerodynamic drag in glow discharge and slight changes in the drag in filamentary discharge. Nonetheless, simultaneous initiation of numerous filamentary discharges can efficiently be used to reduce the drag.

Of the list of inhomogeneous discharges, a microwave discharge is of the greatest interest; this discharge can be glow-type or filamentary depending on the gas pressure. A filamentary discharge at the model's center, which is directed toward the flow, is the most efficient [5].

The anomalous dynamics of shock waves in a weakly ionized glow-discharge plasma was experimentally investigated in the case of both molecular gases (e.g., air and nitrogen) and monatomic ones, such as argon and xenon [3]. In these experiments, the plasma was formed in the gases at a pressure of 15–30 torr. The plasma electron temperature was usually several electron-volts for a degree of ionization of the order of 10^{-6}–10^{-5}. In certain cases magnetic fields (either a longitudinal field or that transverse in relation to the direction of propagation of a shock wave) were used to investigate the influence of charged particles on the dynamics of shock waves. In particular, abnormally high velocities of propagation of a shock wave were observed in the plasma medium simultaneously with a substantial dispersion and the attenuation of the wave.

In [6], ion wind on a flat plate was used for a small reduction in the drag (of approximately 5%) in the turbulent boundary layer for longitudinal Reynolds numbers of $\sim 10^6$. For lower Reynolds numbers ($\sim 10^5$), it became possible to reduce the viscous drag of flow by 50% using a corona discharge between spaced fine wires on a flat surface for both a direct current and an alternate current of low frequency (60 Hz) [7]. The use of each method is limited by the low Reynolds numbers, since it is difficult to evaluate the influence of a corona discharge on high flow velocities.

Plasma actuators can be created on the basis of different atmospheric-pressure discharges: a corona discharge, a dielectric barrier discharge, and a homogeneous glow discharge. These configurations of electric discharges were

A. V. Luikov Heat and Mass Transfer Institute, National Academy of Sciences of Belarus, 15 P. Brovka Str., Minsk, 220072, Belarus. Translated from Inzhenerno-Fizicheskii Zhurnal, Vol. 81, No. 1, pp. 55–61, January–February, 2008. Original article submitted September 27, 2007.

1062-0125/08/8101-0055

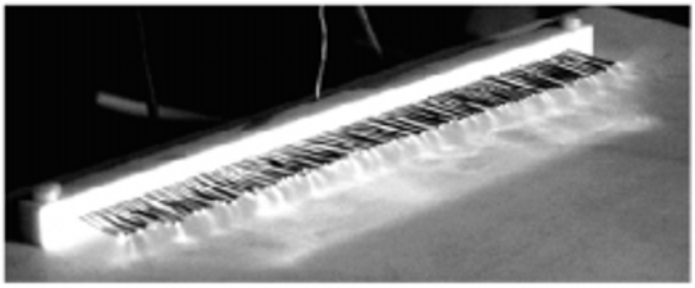

Fig. 1. Photograph of the upper electrode at the instant of discharge.

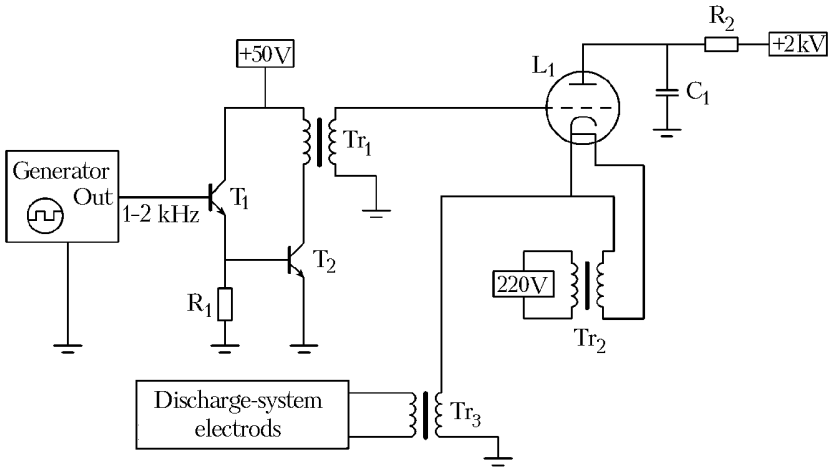

Fig. 2. Diagram of the power supply unit: Tr_1, Tr_2, and Tr_3, transformers; T_1 and T_2, transistors; R_1 and R_2, resistors; C_1, capacitor; L_1, tiratron.

used for reduction in the drag [7–9], back reduction in the flow in turbines and in other internal aerodynamic devices [10–12], back reduction in the flow on the helicopter wings and blades and in other external aerodynamic devices [13, 14], and for modification of the shock-wave front in passage through a sound barrier [15]. The use of plasma actuators makes it possible to ensure a purely electrodynamic linkage between the electric field in the plasma and the neutral gas in the boundary layer [16]. This linkage is sufficiently strong to produce aerodynamically important effects, including the increase or decrease in the aerodynamic drag on a flat plate [17, 18], rearrangement of the flow near the wing at high angles of attack [19], and peristaltic induction of a neutral gas flow by a moving electrostatic wave on the surface in flow [20].

In this work, we have described the methods of obtaining a surface high-frequency barrier discharge and have given the results of investigation of the influence of this discharge on the characteristics of the dynamic boundary layer on a flat surface.

Experimental Equipment and Measurement Methods. The object under study represented a 5-mm-thick smooth plate manufactured from an insulating material (Teflon). Electrodes were installed 2 cm apart on both sides of the plate; one electrode was manufactured in the form of a set of interconnected needles arranged with a step of 2 mm, whereas the other, in the form of a conductor strip, was below the plate (Fig. 1). The electric supply circuit ensuring a high-frequency glow barrier discharge on the electrodes is shown in Fig. 2. Induced ionized-air flow forming the dynamic boundary layer on the plate occurred on the electrodes, when high-voltage pulses were applied.

The structure of the dynamic boundary layer was investigated by the methods of smoke and track visualization. The ion-wind velocity was measured by the mathematical-pendulum method [21]. A diagram of measurement of the velocity and track visualization of the induced flow is given in Fig. 3.

The flow velocity can be calculated from the formula

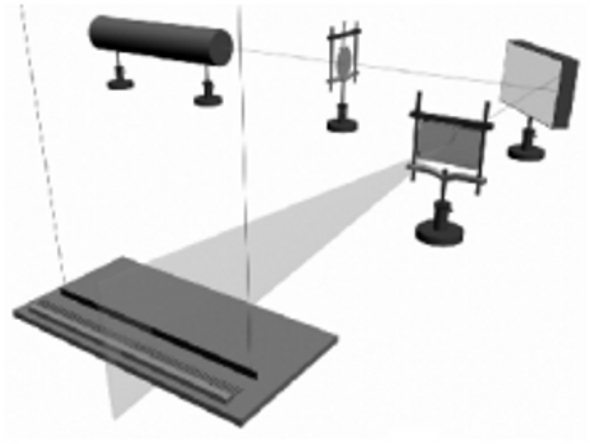

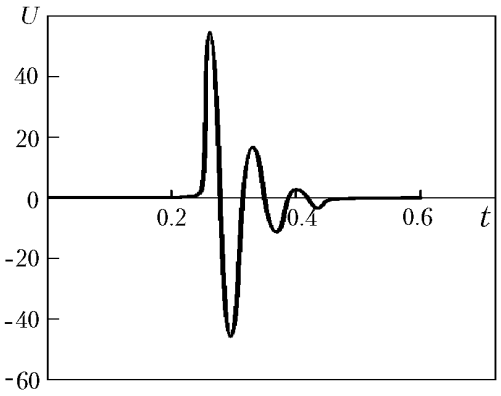

Fig. 3. Diagram of the setup for measurement of the induced-flow velocity.

Fig. 4. Oscillogram of an electric pulse applied to the electrodes. *U*, kV; *t*, msec.

$$V = \sqrt{\frac{2mgl}{\rho LS}} \ .$$

It should be noted that this method makes it possible to just qualitatively evaluate the velocity of the discharge-induced flow because of the disturbances introduced into the flow by the measuring body, since the actual character of collisions is disregarded in the computational formula and all collisions of particles with the measuring plate are described as absolutely elastic ones. Furthermore, during the measurements, the velocities are averaged over the entire area of the measuring plate.

Measurement Results and Their Discussion. The voltage applied to the electrodes was monitored using a resistive divider and a digital oscilloscope. The amplitude value of the voltage varied within 40–120 kV during the experiments. The characteristic oscillogram of a voltage pulse is presented in Fig. 4. The pulse-repetition frequency varied from 0.4 to 1.6 kHz.

Visualization of the flow induced was carried out by the knife-and-slit method on an IAB-451 shadow device. Figure 5 gives the shadow photograph of the induced flow. As follows from the figure, the boundary layer is pressed to the plate, which is due to the influence of the maximum in the lateral flow-velocity distribution, which is located opposite the needles' point.

Figure 6 gives the shadow photograph of the induced flow with a measuring area, which shows that the presence of this area causes a strong disturbance of the flow, followed by the separation of the boundary layer. Thus, the use of the mathematical-pendulum method makes it possible to just qualitatively evaluate the flow velocity average over the boundary layer.

The use of the shadow device prevents direct visualization of the structure of the dynamic boundary layer. The optical inhomogeneity visible with it results from the heating of air by an electric discharge and the appearance of free electrons in the induced flow and of NO_x-, O_x-, and CO_x-type radicals formed in electric discharge in air. Therefore, visualization of the flow structure was also carried out using the laser-knife method upon the introduction of light-reflecting particles or small portions of smoke into the flow.

The results of the track and smoke visualization of the boundary layer are given in Figs. 7 and 8. As follows from Fig. 7, the boundary layer formed is turbulent. A recirculation flow zone due to the presence of inverse-voltage half-periods in supply pulses is observed in the region between two electrodes. The ejection of accelerated particles into the boundary layer is observed at the end of the recirculation zone.

Figures 9 and 10 show the average velocities of the induced flow as functions of the amplitude of voltage applied to the electrodes, the current strength in the discharge, and the repetition frequency of high-voltage pulses. As

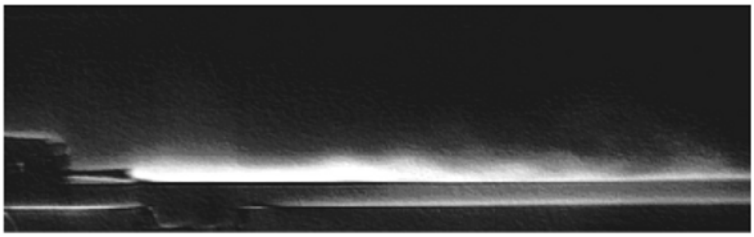

Fig. 5. Shadow photograph of the discharge-induced flow.

Fig. 6. Shadow photograph of the induced flow in measuring the velocity by the mathematical-pendulum method.

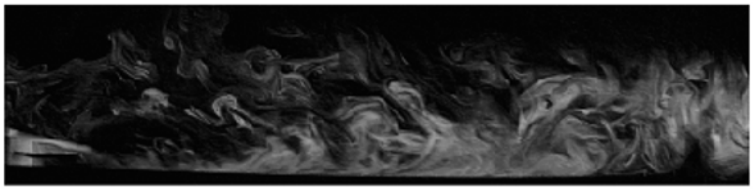

Fig. 7. Smoke visualization of the induced flow.

Fig. 8. Visualization of the induced flow upon the introduction of light-reflecting particles into the flow.

is seen from the plots, the induced-flow velocity attains saturation with growth in the electrical parameters of the discharge. Furthermore, filamentary structures of higher-than-average luminance are observed, as the discharge voltage grows. They result from the contraction of the discharge, once a certain critical value of the discharge-current density has been attained, and represent channels of higher-than-average electrical conductivity, which shunt the basic discharge. The appearance of such structures is an obstacle to further growth in the induced-flow velocity.

The character of the dependence of the flow velocity on the current strength in the discharge is well approximated by a polynomial of the fifth degree

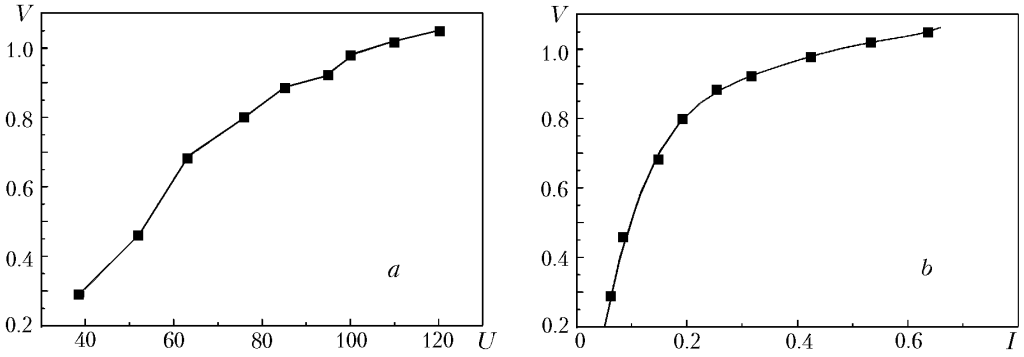

Fig. 9. Velocity of the discharge-induced flow vs. discharge voltage (a) and current strength for the frequency f = 1 kHz (b) (curve, approximation result). V, m/sec; U, kV; I, mA.

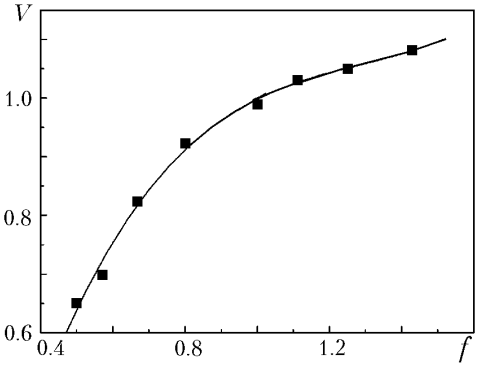

Fig. 10. Velocity of the discharge-induced ion wind vs. discharge frequency (curve, approximation result). V, m/sec; f, kHz.

$$V = -0.30831 + 12.65269I - 55.39148I^2 + 126.96621I^3 - 45.36614I^4 + 65.71322I^5 .$$

An analysis of the dependence of the velocity of the discharge-induced ion wind on the discharge frequency for fixed values of voltage U = 100 kV and current strength I = 0.0319 A has shown that this dependence is well approximated by a polynomial of the third degree:

$$V = -0.43982 + 3.18242f - 2.35426f^2 + 0.61012f^3 .$$

Conclusions. The investigations carried out have shown that a high-frequency barrier discharge formed near the surface in flow can successfully be used in technical devices intended to reduce the aerodynamic drag of aircraft. The gas-discharge plasma is fairly rigidly bound to the electrodes and is virtually not blown away by the incident flow. The formation of filamentary structures in the discharge leads to a limitation of the maximum velocity of the induced flow and a reduction in the operating efficiency of the device. This effect can be minimized by selection of the appropriate dielectric and the size of the interelectrode gap. Furthermore, the formation of filamentary structures in the discharge is prevented by the presence of the external flow; therefore, in the case of blowing of the discharge gap its operating efficiency is considerably improved.

NOTATION

f, pulse-repetition frequency, kHz; g, free-fall acceleration, m/sec^2; I, current strength in the discharge, A; l, displacement of the measuring plate under the action of the incident flow, m; L, filament length, m; m, mass of the measuring plate, kg; M, Mach number; S, area of the measuring plate, m^2; t, time, m/sec; U, voltage between the

electrodes, kV; V, velocity of the discharge-induced flow, m/sec; ρ, air density, kg/m^3. Subscripts: x, stoichiometric coefficient.

REFERENCES

1. P. Bletzinger, B. N. Ganguly, D. Van Wie, and A. Garscadden, Plasmas in high speed aerodynamics, *J. Phys. D: Appl. Phys.*, **38**, R33–R57 (2005).
2. R. B. Miles, S. O. Macheret, M. N. Shneider, C. Steeves, R. C. Murray, T. Smith, and S. H. Zaidi, Plasma-enhanced hypersonic performance enabled by MHD power extraction, in: *Proc. 43rd AIAA Aerospace Sciences Meeting and Exhibit*, Reno, NV, 10–13 January 2005, *Paper AIAA* 2005-0561.
3. R. Appartaim, E. D. Mezonlin, and J. A. Johnson, Turbulence in plasma-induced hypersonic drag reduction, Laboratory for Modern Fluid Physics Center for Nonlinear and Nonequilibrium Aeroscience Florida A&M University, Tallahassee, FL 32310, USA.
4. J. R. Roth, D. M. Sherman, and S. P. Wilkinson, Boundary layer flow control with a one atmosphere uniform glow discharge surface plasma, *AIAA Paper* 98-0328 (1998).
5. T. Xiujun, J. D. Mo, A. S. Chow, and K. X. He, Weakly ionized gas characterization and applications in shear flow control by microwave, in: *Proc. 33rd Plasmadynamics and Lasers Conf.*, 20–23 May 2002, Maui, Hawaii (2002).
6. M. R. Malik, L. M. Weinstein, and M. Y. Hussani, Ion wind drag reduction, *AIAA Paper* 83-0231 (1983).
7. S. El-Khabiry and G. M. Colver, Drag reduction by dc corona discharge along an electrically conductive flat plate for small Reynolds number flow, *Phys. Fluids*, **9**, Issue 3, 587–599 (1997).
8. M. Fulgosi, A. Soldati, and S. Banerjee, Turbulence modulation by an array of large-scale streamwise structures of EHD origin, in: *Proc. FEDSM 99 3rd ASME/JSME Joint Fluids Engineering Conf.*, 18–23 July 1999, San Francisco, CA (1999), pp. 1–8.
9. D. A. Lacoste, D. Pai, and C. O. Laux, Ion wind effects in a positive dc corona discharge in atmospheric pressure in air, in: *Proc. 42nd Aerospace Sciences Meeting and Exhibit*, Reno, NV, 5–8 January 2004, *AIAA Paper* 2004-0354.
10. R. Rivir, L. A. White, C. Carter, B. Ganguly, A. Forelines, and J. Crafton, Turbine flow control, plasma flows, in: *Proc. 41st AIAA Aerospace Sciences Meeting & Exhibit*, Reno, NV, 6–9 January 2003, *AIAA Paper* 2003-6055.
11. A. Asghar and E. J. Jumper, Phase synchronization of vortex shedding from multiple cylinders using plasma actuators, in: *Proc. 41st AIAA Aerospace Sciences Meeting & Exhibit*, Reno, NV, 6–9 January 2003, *AIAA Paper* 2003-1028.
12. L. List, A. R. Byerley, T. E. McLaughlin, and R. D. Van Dyken, Using a plasma actuator to control laminar separation on a linear cascade turbine blade, in: *Proc. 41st AIAA Aerospace Sciences Meeting & Exhibit*, Reno, NV, 6–9 January 2003, *AIAA Paper* 2003-1026.
13. M. L. Post and T. C. Corke, Separation control on high angle of attack airfoil using plasma actuators, in: *Proc. 41st AIAA Aerospace Sciences Meeting & Exhibit*, Reno, NV, 6–9 January 2003, *AIAA Paper* 2003-1024.
14. L. S. Hultgren and D. E. Ashpis, Demonstration of separation delay with glow-discharge plasma actuators, in: *Proc. 41st AIAA Aerospace Sciences Meeting & Exhibit*, Reno, NV, 6–9 January 2003, *AIAA Paper* 2003-1025.
15. S. Leonov, D. Yarantsev, A. Kuryachii, and A. Yuriev, Study of friction and separation control by surface plasma, in: *Proc. 42nd Aerospace Sciences Meeting and Exhibit*, Reno, NV, 5–8 January 2004, *AIAA Paper* 2004-0512.
16. C. Liu and J. R. Roth, Atmospheric glow discharge plasma for aerodynamic boundary layer control, in: *Proc. 21st IEEE Int. Conf. on Plasma Science*, 6–8 June 1994, Santa Fe, NM, ISBN 7803-2006-9, pp. 97–98, Paper IP-26.
17. J. R. Roth, D. M. Sherman, and S. P. Wilkinson, Electrohydrodynamic flow control with a glow-discharge surface plasma, *AIAA J.*, **38**, No. 7, 1166–1172 (2000).

18. H. Sin, A polyphase power supply and peristaltic flow accelerator using a one atmospheric uniform glow discharge plasma, *M. S. in Electrical Engineering Thesis*, Department of Electrical and Computer Engineering, University of Tennessee, Knoxville (2002).
19. J. R. Roth, H. Sin, R. C. M. Madhan., and S. P. Wilkinson, Flow re-attachment and acceleration by paraelectric and peristaltic electrohydrodynamic (EHD) effects, in: *Proc. 41st AIAA Aerospace Sciences Meeting & Exhibit*, Reno, NV, 6–9 January 2003, *AIAA Paper* 2003-0351.
20. J. R. Roth, Aerodynamic flow acceleration using paraelectric and peristaltic electrohydrodynamic (EHD) effects of a one atmosphere uniform glow discharge plasma (OAUGDP), *Phys. Plasmas*, **10**, No. 5 (2003).
21. R. Hudlestone and S. M. Leonard (Eds.), *Plasma Diagnostic Techniques* [Russian translation], Mir, Moscow (1967).